A Computational Study of Feedback Effects on Signal Dynamics in a Mitogen-Activated Protein Kinase (MAPK) Pathway Model

Anand R. Asthagiri* and Douglas A. Lauffenburger

Department of Chemical Engineering, Massachusetts Institute of Technology, Cambridge, Massachusetts

Exploiting signaling pathways for the purpose of controlling cell function entails identifying and manipulating the information content of intracellular signals. As in the case of the ubiquitously expressed, eukaryotic mitogen-activated protein kinase (MAPK) signaling pathway, this information content partly resides in the signals' dynamical properties. Here, we utilize a mathematical model to examine mechanisms that govern MAPK pathway dynamics, particularly the role of putative negative feedback mechanisms in generating complete signal adaptation, a term referring to the reset of a signal to prestimulation levels. In addition to yielding adaptation of its direct target, feedback mechanisms implemented in our model also indirectly assist in the adaptation of signaling components downstream of the target under certain conditions. In fact, model predictions identify conditions yielding ultra-desensitization of signals in which complete adaptation of target and downstream signals culminates even while stimulus recognition (i.e., receptor−ligand binding) continues to increase. Moreover, the rate at which signal decays can follow first-order kinetics with respect to signal intensity, so that signal adaptation is achieved in the same amount of time regardless of signal intensity or ligand dose. All of these features are consistent with experimental findings recently obtained for the Chinese hamster ovary (CHO) cell lines (Asthagiri et al., *J. Biol. Chem.* **1999**, *274*, 27119−27127). Our model further predicts that although downstream effects are independent of whether an enzyme or adaptor protein is targeted by negative feedback, adaptor-targeted feedback can "back-propagate" effects upstream of the target, specifically resulting in increased steady-state upstream signal. Consequently, where these upstream components serve as nodes within a signaling network, feedback can transfer signaling through these nodes into alternate pathways, thereby promoting the sort of signaling cross-talk that is becoming more widely appreciated.

Introduction

Upon recognition of external stimuli, cell surface receptors initiate a network of intracellular signaling pathways, which directly govern cell behavior. These intracellular signals are critical for coordinating biological processes at cellular, tissue, and whole-organism levels, and aberrations among them often yield severe pathologies such as the development of cancer (Joneson and Bar-Sagi, 1997; Maemura et al., 1999). Therefore, signal transduction mechanisms have been identified as potentially powerful targets for disease therapy (Levitzki, 1996). In devising rational approaches in such applications, solely identifying appropriate molecular targets among the signaling machinery is not sufficient. Additionally, the degree to which signals—more specifically, their information content—need to be tuned or adjusted must also be assessed quantitatively (Asthagiri and Lauffenburger, 2000).

Often this information content resides within signals' dynamics rather than their steady-state properties. This is especially evident in the case of information propagation via the eukaryotic mitogen-activated protein kinase (MAPK) signaling pathway, which culminates with the activation of a family of signaling enzymes known as extracellular signal-regulated kinases (ERKs) (Lewis et al., 1998; Roovers and Assoian, 2000). In certain cells, some stimuli elicit only a transient activation of ERKs with the signal rapidly undergoing complete adaptation, a term referring to the fact that the signal essentially resets or returns to its prestimulation steady-state level (Koshland et al., 1982). Importantly, adaptation does not imply abrogation of function. We have demonstrated elsewhere that transient activation of ERK2 in Chinese hamster ovary (CHO) cells governs DNA synthesis response (Asthagiri et al., 2000), and in the simplest scenario of stimulation solely by cell adhesion to extracellular matrix, the degree of response is strictly proportional to the intensity of transient signal. Consistent with these findings, correlative evidence in other cell types suggests that transient ERK1/2 activation promotes cell proliferation, while sustained activation leads to differentiation (Marshall, 1995). For example, in hepatocytes and PC12 cells, forcing sustained activation of ERK1/2 inhibits DNA synthesis, while transient ERK1/2 activation promotes this response (Tombes et al., 1998).

However, the association between transient ERK1/2 activation and proliferation may not be uniform in all cell types. It has been shown that sustained ERK1/2 activation is required for upregulation of cyclin D1 in

* To whom correspondence should be addressed; presently at the Department of Cell Biology, Harvard Medical School, Boston, MA. Tel: 617-432-3971. Fax: 425-944-7506. E-mail: anand_asthagiri@hms.harvard.edu.

10.1021/bp010009k CCC: $20.00
Published on Web 03/02/2001

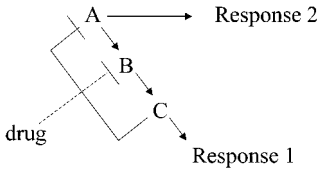

Figure 1. Ancillary effects due to negative feedback. Signaling pathway A → B → C leads to Response 1. C feeds back to inhibit A, thereby constraining A's effect on Response 2. In the presence of a drug designed to attenuate Response 1 via inhibition of B, the drug would also reduce signaling via C and weaken feedback inhibition of A, thereby indirectly increasing Response 2.

certain fibroblasts (Roovers et al., 1999), which is one step in the eventual hyperphosphorylation of pRb, its dissociation from E2F, and E2F-mediated upregulation of cyclin A expression (DeGregori et al., 1995; Schulze et al., 1996). Since cyclin A upregulation is required for entry into S phase (Girard et al., 1991), this finding suggests that sustained, and not transient, ERK1/2 activation is essential to promote DNA synthesis in these cells.

While previous work has been devoted to steady-state effects (Ferrell, 1996; Huang and Ferrell, 1996), the above body of literature indicates that important information resides at least partly in ERK signaling dynamics (i.e., its transient versus sustained character) albeit the precise consequence may be dependent on cell type. In addition to stimulatory mechanisms that initiate and propagate signal through the MAPK pathway, its balance with negative regulatory elements will determine whether the signal undergoes adaptation and what degree of adaptation occurs. Therefore, rationally adjusting the information content of ERK signals in order to tune cell response will require an understanding of how particular modes of negative regulation influence signaling dynamics of this pathway.

These modes of negative regulation are often contained within feedback loops, thereby providing autonomous regulation of signaling pathways. While such feedback regulation may be beneficial for controlling signal propagation within a cell, these mechanisms may confound interpretation of experimental results if they are strictly viewed with a bias toward an "outside-in", unidirectional flow of signal. For example, in the simplified schematic presented in Figure 1, inhibition of species B would result in attenuation of feedback driven by C, thereby resulting in prolonged and/or increased signaling via A. Under such inhibition, not only would response 1 be reduced, but also an ancillary effect may be to enhance response 2, even though the second response is not under direct regulation by B or C. Therefore, even the fundamental task of ascribing functional significance to individual proteins, a significant focus of the post-genomic era (Kao, 1999), will require better understanding of how feedback mechanisms impart previously unpredicted roles for familiar proteins in cell behavioral regulation.

In this present work, our aim is to develop a mathematical model based on the MAPK pathway in order to investigate how putative negative regulatory mechanisms, particularly those under feedback control, affect signal propagation. We will compare model predictions to our experimental findings, not with the intent of manipulating model parameters to fit experimental data but rather to assess how different modes of feedback affect more general properties of ERK signaling dynamics such as the attainment of adaptation.

Background: MAPK Pathway. In the most general framework, signal activation through the MAPK pathway

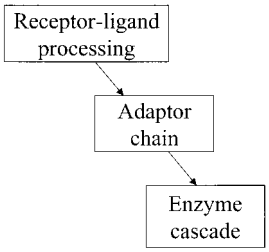

Figure 2. Modules involved in signal propagation via the MAPK pathway. The events leading from stimulus recognition at the cell surface to activation of ERKs are represented by three sequential modules. In the first module, receptor−ligand interaction is followed by other signal processing events such as dimerization and receptor autophosphorylation. The second module involves events such as the physical engagement of an activated receptor−ligand complex with a series of adaptors, producing an adaptor chain. Finally, the terminal constituents of the adaptor chain propagate signal into an enzyme cascade, which leads eventually to the activation of ERKs and other downstream kinases that directly control cell function.

is achieved by a three-step scheme that forms the basis for our model (Figure 2). We first provide an overview of these signal-activating mechanisms, before broaching the topic of negative regulation in this pathway. In the first step, receptor−ligand binding and post-ligand occupancy events such as dimerization or aggregation of multiple receptor−ligand complexes culminate in the eventual association of an adaptor protein with the activated form of the receptor (van der Geer and Hunter, 1994). The simplest example would involve the binding of a growth factor to its receptor, consequent dimerization-induced phosphorylation of the receptor, and its association with an adaptor protein such as Shc.

This initial adaptor protein then instigates a series of physical binding steps resulting in the recruitment of other adaptor proteins. Continuing our example, phosphorylation of Shc would enable recruitment of Grb2, whose SH3 domains bind to the next protein in the cascade Sos (Rozakis-Adcock et al., 1993). The number of adaptor proteins following receptor recognition of stimulus can vary widely. In the case of integrin-mediated adhesion, aggregated, ligand-bound integrins recruit focal adhesion kinase (FAK), which in turn may associate directly with Grb2-Sos or indirectly by first binding to Cas. While some domains in Cas bind directly to Grb2, yet others associate with Crk and thereby indirectly connect to Grb2. Thus, a chain containing as few as two (FAK-Grb2) or as many as four (FAK-Cas-Crk-Grb2) proteins can link integrins to Sos via FAK (Hanks and Polte, 1997).

The final step in this cascade of protein associations is the recruitment of Sos, which serves as a guanine nucleotide exchange factor (GNEF) for Ras. Sos converts Ras from its GDP-bound, inactive state to a GTP-bound, active configuration; importantly, this conversion is enabled only when Sos is recruited to the membrane through its interactions with adaptor proteins (Aronheim et al., 1994). Reverse enzymes known as GTPase activating proteins (GAPs) stimulate the intrinsic GTPase capability of Ras, which hydrolyzes Ras-bound GTP to GDP, essentially recycling Ras back to its inactive state. The balance between GNEF and GAP activity determines the fraction of active Ras. Among the many effectors for Ras is a serine/threonine kinase Raf that is activated by recruitment to the membrane via physical association with membrane-bound active Ras (Mineo et al., 1997). While it is unclear precisely how Raf enzymatic activity is stimulated, the current paradigm is that Ras serves

to localize Raf to the membrane where preexisting enzymes activate Raf, perhaps via phosphorylation (Leevers et al., 1994; Stokoe et al., 1994). Once activated, Raf commences a kinase cascade resulting in the activation of MEK and ERK (Lewis et al., 1998). The steps from Sos to the activation of ERK may be viewed predominantly as an enzyme cascade; with the exception of Raf activation (wherein Ras may be involved more as a "docking" protein than a catalyst), each step in this series of post-Sos events involves the functionality of activating enzymes (e.g., GNEF or kinase) in balance with deactivating enzymes (e.g., GAP or phosphatase).

Through this general framework involving receptor−ligand binding events, an adaptor chain, and an enzyme cascade, recognition of a stimulus is propagated to the eventual activation of ERK1/2. Activated ERKs proceed to activate other downstream kinases such p90 Rsk-1 and Rsk-2, MAPKAP 2 and 3, and Mnks 1 and 2 (Davis, 1993). In addition, ERK1/2 phosphorylate and modify the activity of several nuclear transcription factors such as c-Fos, c-Myc, and those belonging to the Ets family (e.g., Elk-1). Finally, ERK1/2 also regulate cytoskeletal proteins (e.g., microtubule-associated proteins 1 and 2) and proteins involved in other signaling pathways (e.g., $cPLA_2$). Because of its ability to activate a range of downstream targets, ERK1/2 controls numerous cell processes such as proliferation, migration, differentiation, and gene expression.

While the above discussion outlines mechanisms utilized to transfer information from stimulus to response, there are also several modes of negative regulation opposing signal propagation, some of which perform within feedback loops. First, the aforementioned deactivating enzymes, such as GAPs that activate intrinsic GTPase activity of Ras, counter activation mechanisms. Other examples include phosphatases such as dual specificity phosphatases MKP-1, MKP-2, MKP-3, and PAC-1 (Keyse, 2000; Lewis et al., 1998) that catalyze direct deactivation of ERKs by dephosphorylation of its tyrosine and threonine residues. These deactivating enzymes may be present in fixed quantities even when stimulus is first being detected and therefore may be competing with signal propagation from its inception. However, in some instances, expression of phosphatases has been shown to be upregulated in response to signaling through the MAPK pathway in a form of feedback that typically operates over an extended time scale as a result of its reliance on transcription of the negative regulator (Brondello et al., 1997; Grumont et al., 1996).

In contrast, other negative regulatory pathways perform via feedback control over a shorter time scale. These feedback mechanisms disconnect the sequence of pathways that link stimulus recognition to ERK1/2 activation. Several such decoupling mechanisms have been reported that target both adaptor proteins and enzymes upstream of ERKs, including serine/threonine phosphorylation of a proline-rich carboxy-terminal domain of Sos, hyperphosphorylation of Raf, and phosphorylation on two threonine residues of MEK (Brunet et al., 1994; Buday et al., 1995; Langlois et al., 1995; Wartmann et al., 1997). These covalent modifications of Sos, Raf, and MEK shift these proteins into a signaling-defective state. For example, phosphorylation of serine/threonine residues on Sos has been implicated in dissociating Sos from Grb2 (Langlois et al., 1995) or dissociating the Grb2-Sos complex from the phosphorylated receptor (Buday et al., 1995), thereby disengaging the ability of hyperphosphorylated Sos to remain at the membrane and perform its Ras-activating signaling function.

In this manner, signal-activating reactions and several negative regulatory mechanisms, involving both direct (e.g., phosphatases) and indirect/decoupling modes with some operating via feedback, regulate signal propagation via the MAPK pathway. Better understanding of how components and mechanisms of this pathway cumulatively determine signal dynamics may offer strategies for rationally manipulating these dynamics and consequently cell behavior. For this purpose, a mathematical model has been developed to investigate the role of putative negative regulatory mechanisms in signal propagation via the MAPK pathway.

Model Description

Activation Mechanisms. We formalize the above description of the MAPK pathway into a model schematic depicted in Figure 3. The receptor−ligand events involve the minimal steps necessary to produce an activated receptor−ligand complex. Specifically, the ligand (L) binds to receptor (R) with an association and dissociation rate constant (k_f and k_r, respectively). Once ligand-occupied receptors (C) interact to form a dimer (C_2) and as a result become phosphorylated to yield an activated form of the receptor (C*), they are able to associate with the first intracellular signaling molecule, an adaptor protein (A_1). This complex (C^*A_1) then associates with a second adaptor protein (A_2) to form a larger complex (E_0^*). Both adaptors may also precouple within the cytosol (analogous to Grb2 and Sos) in the absence of any stimulus to form a cytosolic heteroadaptor complex (A_1A_2). This preformed complex may also directly interact with an activated receptor complex (C*) to form E_0^*.

It is assumed that localization of the second adaptor protein (A_2) to a membrane-bound state (E_0^*) activates the enzymatic functionality of A_2. This activation may occur as a result of allosteric regulation, wherein association of the second adaptor protein with the complex C^*A_1 changes its configuration to expose and/or activate a catalytic site necessary for interaction with its substrate E_1. Alternatively, the substrate E_1 may be preassociated with the plasma membrane, and localization of the second adaptor to the membrane may confer access to its substrate, in a manner analogous to the Sos-Ras interaction. While the details are not considered, the supposition is that the second adaptor A_2 can convert its substrate E_1 to its active form (E_1^*) only when the second adaptor resides in the signaling complex E_0^* and not in its unbound state A_2 or in its heterodimer form A_1A_2. Once the substrate E_1 is converted to its active state E_1^*, it initiates a cascade of enzyme activation steps (analogous to Raf-MEK-ERK-ERK substrate cascade) in which each enzyme (E_i) is converted to its active form (E_i^*) only by its active predecessor (E_{i-1}^*) by the following elementary steps:

$$E_{i-1}^* + E_i \leftrightarrow E_iE_{i-1}^* \rightarrow E_{i-1}^* + E_i^* \qquad (1)$$

with rate constants k_i^+ and k_i^- describing the association and dissociation of E_{i-1}^* and E_i and the rate constant $k_{i,cat}$ assigned to the first-order conversion of the transition complex $E_iE_{i-1}^*$ into products E_{i-1}^* and E_i^*. The amount of final enzyme E_5^* in its active state is considered the output of the signaling pathway in response to stimulation by a certain concentration of ligand L.

Negative Regulatory Elements Independent of Feedback Control. There are two negative regulatory elements that operate constitutively and are therefore implemented in the base schematic, even without con-

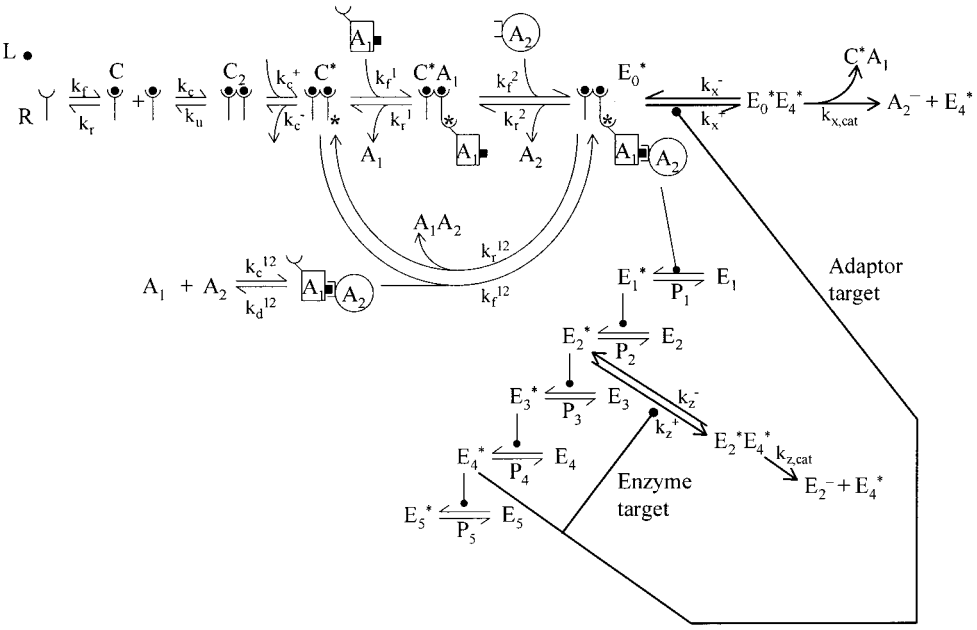

Figure 3. Model schematic. This scheme is based on mechanisms prevalent in the MAPK signaling pathway and describes the species and interactions included in the mathematical model. A detailed discussion of signal flow through the delineated pathway is provided in the Model Description section.

Table 1. Dimensionless Variables

dimensionless variable and description	normalization factor
time, τ	$1/k_r$
free ligand, l	L_0
free receptor, r ligand-bound receptor, c ligand-bound and dimerized receptor, c_2 dimerized and activated receptor, c^*	R_0
free first adaptor, a_1 active receptor−ligand dimer:adaptor 1 complex, c^*a_1 adaptor heterodimer, a_1a_2	A_1^T
free second adaptor, a_2 receptor−ligand dimer:adaptors 1 + 2 complex, e_0^* nonfunctional second adaptor, a_2^-	A_2^T
transition complexes in feedback mediated by enzyme E_4^*, $e_0^*e_4^*$ and $e_2^*e_4^*$	E_4^T
inactive signaling enzyme, e_i activated signaling enzyme, e_i^* transition complex between an inactive substrate and its activator, $e_ie_{i-1}^*$	E_i^T
deactivating enzyme, p_i transition complex between an active substrate and its deactivating enzyme, $e_i^*p_i$	P_i^T
nonfunctional second enzyme, e_2^-	E_2^T

sideration of negative feedback mechanisms. First, each protein−protein association has a complementary dissociation reaction as described in Figure 3. Second, each active enzyme (E_i^*) in the enzyme cascade is deactivated by its corresponding deactivating enzyme (P_i) through the following elementary steps:

$$E_i^* + P_i \leftrightarrow E_i^*P_i \rightarrow E_i + P_i \qquad (2)$$

with rate constants $k_{P_i}^+$, $k_{P_i}^-$, and k_{cat,P_i} assigned in a manner analogous to eq 1.

Modes of Negative Feedback. Focusing our attention on the adaptor chain and enzyme cascade, we implement two major modes of intrapathway feedback operating within the time scale of activation steps based on known mechanisms in cellular systems. The difference between mechanisms lies in the choice of element serving as the target of feedback, either a species in the adaptor chain or the enzyme cascade. We select the source or feedback initiator to be the active form of an enzyme late in the cascade, specifically E_4^*, on the basis of the fact that most modes of known feedback in the MAPK pathway emanate from kinases late in the pathway such as ERK1/2 (Anderson et al., 1991; Brunet et al., 1994; Corbalan-Garcia et al., 1996).

In adaptor-targeted feedback, active enzyme E_4^* directly catalyzes covalent modification of those second adaptor proteins A_2 existing in the active complex E_0^*. This modification is assumed to convert A_2 into an inactive form A_2^-, which is no longer capable of associating with the first adaptor protein A_1. Moreover, this modification of complex-associated, activated A_2 disassembles the existing E_0^* complex into its constituents: C^*A_1 and now inactive A_2^-. This mode of feedback is analogous to the serine/threonine phosphorylation of Sos, which either disengages Sos from the Sos-Grb2 complex (Chen et al., 1996; Langlois et al., 1995) or dissociates the Grb2-Sos complex from activated receptor (Buday et al., 1995). Moreover, consistent with our model scheme, a kinase late in the cascade seems to be involved in negatively regulating Sos. While some of the phosphorylation sites on Sos match consensus target sites of ERK1/2 (Corbalan-Garcia et al., 1996), a kinase downstream of ERK1/2, p90 Rsk-2, has also been implicated in Sos modification (Douville and Downward, 1997).

In addition to an adaptor-targeted feedback regulation, another mode targets enzymes. Raf hyperphosphorylation negatively modulates its plasma membrane localization, thereby attenuating its activity (Wartmann et al., 1997). In this same study, Raf hyperphosphorylation was shown to depend on MEK activation as pharmacological inhibition of MEK relieves negative modulation of Raf. Consistent with these findings, Raf has been implicated as a potential substrate for ERK (Anderson et al., 1991). In addition to Raf, MEK also undergoes feedback phosphorylation driven by ERK (Brunet et al., 1994). In our

Table 2. Parameters and Their Typical Values[a]

parameter	description	value	units
n	cell density	3.3×10^4	cells/mL
L_0	initial ligand concentration	k_r/k_f	M
R_0	initial number of free receptors	10^5	no./cell
A_1^T, A_2^T	total number of each adaptor protein	10^4	no./cell
E_i^T, $i = 1-5$	total number of activating enzymes at stage i	10^4	no./cell
P_i^T, $i = 1-5$	total number of deactivating enzymes at each stage i	5×10^3	no./cell
k_f	receptor−ligand association rate constant	10^7	M^{-1} min^{-1}
k_r	receptor−ligand dissociation rate constant	0.3	min^{-1}
k_c	rate constant for dimerization of ligand-bound receptors	6×10^7	M^{-1} min^{-1}
k_u	rate constant for dissociation of dimers	60	min^{-1}
k_c^+	rate constant for activation of dimerized receptor−ligand complexes	50	min^{-1}
k_c^-	rate constant for deactivation of active receptor−ligand dimers	5	min^{-1}
k_f^1, k_f^2, k_f^{12}, k_c^{12}	association rate constants among adaptors	3×10^8	M^{-1} min^{-1}
k_r^1/k_f^1, k_r^2/k_f^2, k_r^{12}/k_f^{12}, k_d^{12}/k_u^{12}	equilibrium dissociation constant for adaptor interactions	10^{-7}	M
k_i^+, $k_{P_i}^+$, k_x^+, k_z^+	enzyme−substrate association rate constant	6×10^8	M^{-1} min^{-1}
k_i^-, $k_{P_i}^-$, k_x^-, k_z^-	enzyme−substrate dissociation rate constant	30	min^{-1}
$k_{cat,i}$, k_{cat,P_i}, $k_{cat,x}$, $k_{cat,z}$	rate constant for the formation of product from enzyme−substrate transition complex	6	min^{-1}

[a] These parameter values were used in all simulations unless noted otherwise and were derived from the following sources: k_r and k_f (Lauffenburger and Linderman, 1993); k_c and k_u (Haugh and Lauffenburger, 1997; Lauffenburger and Linderman, 1993); k_c^+ and k_c^- (Kholodenko et al., 1999); k_f^1, k_f^2, k_f^{12}, k_c^{12} and k_r^1/k_f^1, k_r^2/k_f^2, k_r^{12}/k_f^{12}, k_d^{12}/k_u^{12} (Haugh and Lauffenburger, 1997; Kholodenko et al., 1999); k^+, k^-, k_{cat} (Levchenko et al., 2000).

model, we incorporate an analogous mode of feedback via the conversion of the active enzyme E_2* into an inactive state E_2^- catalyzed by an active enzyme late in the cascade (E_4*).

A mass-action kinetic model was derived from the described schematic as outlined in the Appendix, and the resulting system of differential equations was solved using the MATLAB "ode23s" subroutine. All variables within the model were nondimensionalized using normalization factors given in Table 1. Table 2 provides descriptions and typical values for model parameters.

Results and Discussion

General Features of Model Behavior. ***Negative Regulatory Elements in the Absence of Feedback.*** Adaptor dissociation from complexes and deactivating enzymes present at each stage of the enzyme cascade negatively influence signal propagation. Yet, these mechanisms alone do not promote adaptation (Figure 4). Rather, upon ligand stimulation, the fraction of enzymes (e^*_i) in its activated form monotonically increases with time until reaching a supra-basal, steady-state value. Moreover, despite signal-countering mechanisms, an overall amplification of signal is observed across the enyzme cascade for the parameters given in Table A2; that is, if we consider the fraction of enzymes in its active form at steady-state ($e^*_{i,ss}$) as a measure of signal strength at each stage, the value of $e^*_{i,ss}$ increases as signal progresses down the cascade.

Such amplification is generally prescribed as one of the functions of enzyme cascades, presumably due to a compounding effect arising from a series of enzyme−substrate interactions wherein an individual upstream enzyme is capable of activating several downstream targets. However, our model shows that signal may be amplified or attenuated as it passes through the cascade, in part depending on the relative levels of signal-generating enzymes and signal-countering deactivators. If we consider an enzyme cascade in which deactivators P_i return active signaling enzymes E_i* to their ground-state E_i, the ratio of total amount of deactivator (P_i^T) to total amount of activator enzymes (E_i^T) determines the balance between attenuation and amplification (Figure 5). For extremely small values of this ratio, deactivator

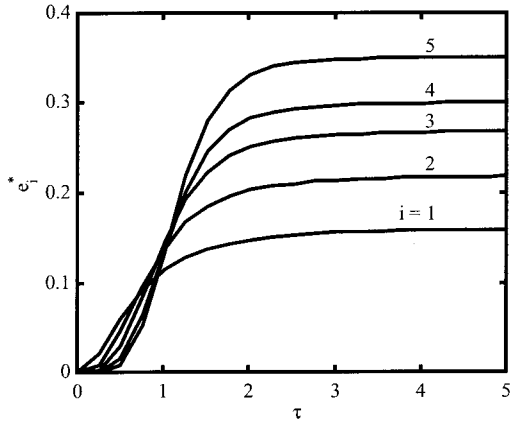

Figure 4. Mechanisms countering signal propagation do not yield adaptation in the absence of feedback control. In the absence of feedback, negative regulatory mechanisms such as dissociation of adaptor protein-containing signaling complexes and deactivator-mediated shut-down of signaling enzymes are unable to induce signal adaptation. Ligand stimulation initiates a monotonic increase in the fraction of enzymes (e_i*) activated at each stage ($i = 1-5$) of the cascade over time. For parameter values shown in Table A2, a net amplification of signal across the cascade is achieved, so that activation of only 15% of E_1 enzymes is sufficient to activate nearly 35% of E_5 enzymes at steady state.

effects are essentially negligible in comparison to the signal-promoting effect of the far more abundant active enzymes E_{i-1}*. Thus, there is no net deactivation of signaling enzymes at each stage, resulting in full conversion of enzyme to its active form E_i* for all i. At intermediary levels of $\log(P_i^T:E_i^T)$ in the range of −1.5 to −0.25, a sufficient amount of deactivator function exists to counter activation of enzymes E_i. However, since signal-promoting enzymes are still in excess of deactivators, the result is net amplification across the cascade. Only when $\log(P_i^T:E_i^T)$ reaches sufficiently high levels (0−0.5), does deactivator functionality become dominant to counter signal-promoting effects of active enzyme E_{i-1}*, yielding signal attenuation at each stage of the cascade. Since the ratio $P_i^T:E_i^T$ is a key determinant for amplification versus attenuation, variations in this ratio among the different stages can produce sporadic shifts in signal strength as information traverses the pathway (Figure 6), demonstrating that kinase cascades such as the

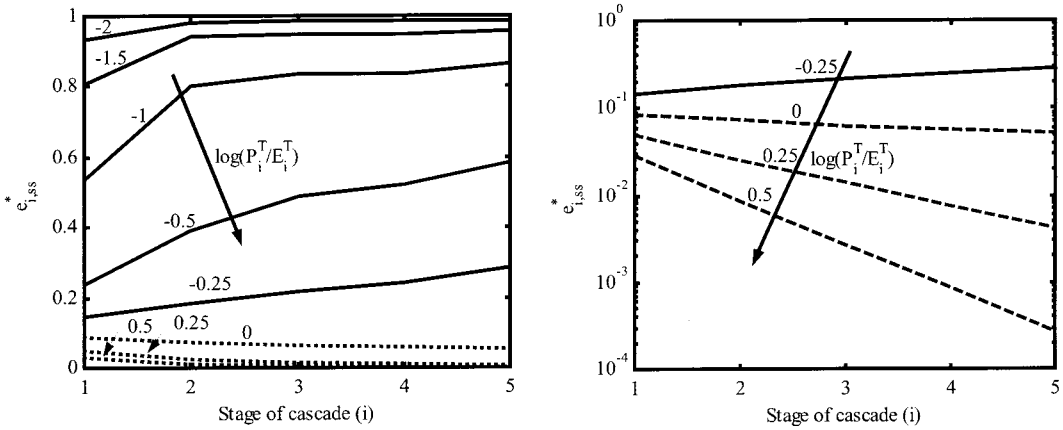

Figure 5. Enzyme cascades may operate as signal amplifiers and attenuators. Signal intensity at the *i*th stage of the cascade is given by the fraction of total enzyme ($e_{i,ss}$*) at that stage maintained in its active form at steady state. A cascade serves as an amplifier if signal intensity increases with stage position and conversely as an attenuator if signal intensity decreases as information progresses down the cascade. Varying the deactivator:activator ratio P_i^T:E_i^T at all stages concurrently determines whether the cascade as a whole functions as a signal amplifier or attenuator.

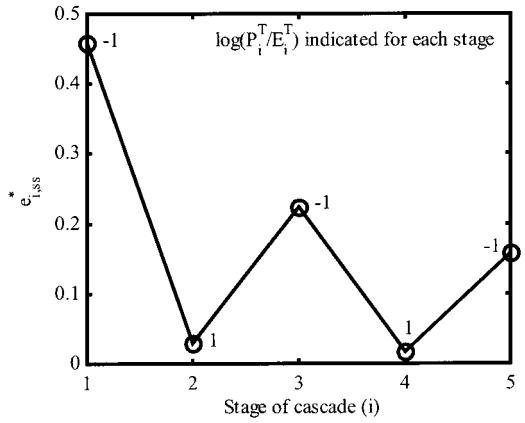

Figure 6. Signal strength may fluctuate across a cascade. If each stage possesses different deactivator:activator ratios as emulated by toggling the value of log(P_i^T:E_i^T) between values of −1 and 1 across the cascade, signal strength shifts sporadically as it progresses through the cascade as the stages alternate between amplification and attenuation modes.

MAPK signaling module are not confined to behave solely as signal amplifiers.

Implementation of Negative Feedback. Feedback emanating from an enzyme late in the cascade (E_4*) and targeting either the adaptor-containing complex E_0* or the activated enzyme E_2* effectively converts the level of E_0* or E_2*, respectively, to a basal level, thereby achieving complete adaptation of these target species (Figure 7A and B). Moreover, complete adaptation of target signal is a robust property, albeit the time for adaptation can vary depending on model parameters (data not shown). Similar robustness of adaptation has been demonstrated for another signaling scheme involving feedback (Alon et al., 1999; Barkai and Leibler, 1997), and it has been shown that robust adaptation holds if the system utilizes integral feedback (Yi et al., 2000).

Importantly, in both adaptor- and enzyme-targeted feedback, adaptation is not limited to the target but propagates through the enzyme cascade, returning all post-target signals to their ground states. While complete adaptation of the target removes impetus for further activation of downstream signals, a reduction in the fraction of downstream signaling enzymes in the active state (e_i* for all *i* greater than target stage) also requires deactivating enzymes at each post-target stage. For example, in the absence of a deactivator in the fifth stage

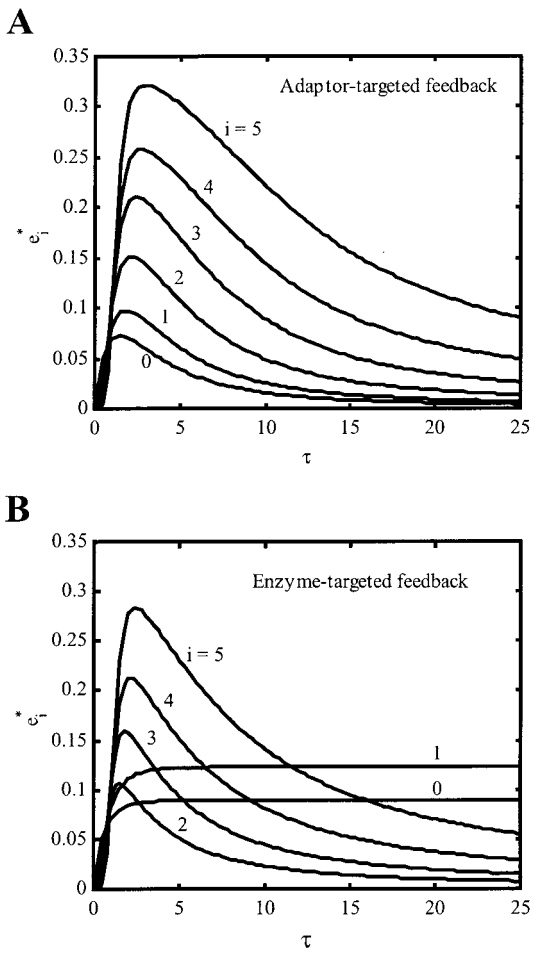

Figure 7. Complete adaptation is achieved for signals downstream of feedback target. At a fixed deactivator:activator ratio, implementation of adaptor-targeted feedback (A) induces adaptation of not only the target signal e_0* but also signals downstream of the target, e_i* for $i = 1-5$. Similarly, enzyme-targeted feedback (B) enables adaptation of the target signal e_2* and signals downstream of the target, but not those signals upstream of the target, e_0* and e_1*.

of the enzyme cascade, a condition approximated by setting the deactivator-to-activator ratio P_5^T:E_5^T for this stage to 10^{-10}, the fraction of active enzyme at that stage (e_5*) fails to decay, although signal level at the previous stage completely subsides (Figure 8).

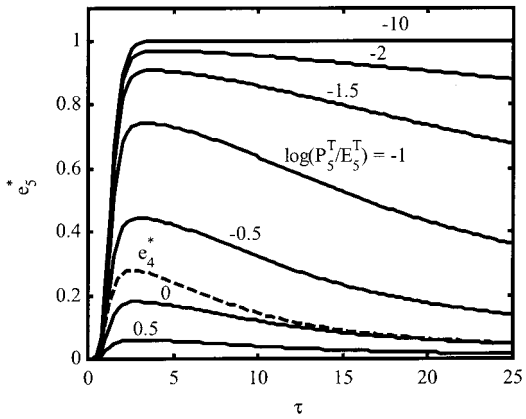

Figure 8. Adaptation of signals downstream of feedback target requires the presence of corresponding deactivator. With the inclusion of adaptor-targeted feedback, the time course of a late signal in the cascade (e_5*) is depicted for variations in the deactivator:activator ratio at this stage. In the presence of deactivator P_5, feedback induces adaptation of signal e_5*, with the time course of adaptation dependent on the ratio P_5^T:E_5^T. However, in the absence of P_5, as approximated by setting log(P_5^T:E_5^T) = −10, adaptor-targeted feedback fails to reduce the level of activated enzyme E_5* within a physiologically meaningful time scale, even though the component directly upstream (E_4*) adapts completely (dotted line).

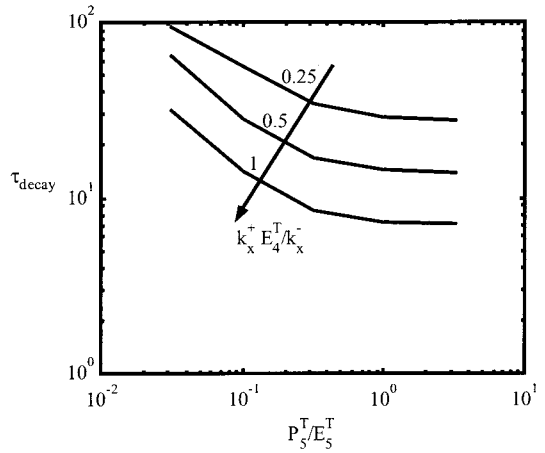

Figure 9. Adaptation kinetics' dependence on the deactivator: activator ratio and feedback strength. The time scale of adaptation is defined as the time required for a signal to decay from its peak activity to its half-maximal level (refer to Figure 8 for a sample time course). For a fixed degree of adaptor-targeted feedback, the time scale of adaptation of signal e_5* is a decreasing function of the ratio P_5^T:E_5^T. Stronger feedback is implemented by increasing the value of the dimensionless group $k_x^+ E_4^T/k_x^-$, which is directly related to the affinity of the feedback initiator E_4* for its target E_0*. For a fixed P_5^T:E_5^T ratio, higher feedback strength reduces the time scale of adaptation.

In addition to propagating signal adaptation, the deactivator-to-activator ratio P_i^T:E_i^T is a key determinant of the time required to achieve adaptation of a post-target signal (Figure 8). We define the time scale for adaptation (τ_{decay}) as the time required for the signal to decay from its peak or maximal activity to half-maximal activity. As depicted in Figure 9, this time scale for adaptation for a given stage (in this case $i = 5$) is a decreasing function of the deactivator-to-activator ratio at that stage. At low values of this ratio, relatively insufficient deactivator P_5 is present to shut off the signaling enzyme E_5*, even though negative feedback has halted further stimulation. As the value of this ratio is increased, deactivator amount rises to a level capable of decaying the E_5* signal within a shorter time scale. However, the time scale of adaptation approaches an asymptotic limit, in part restricted by the degree to which feedback is driven. Increasing feedback strength by raising the value of the dimensionless parameter $k_x^+E_4^T/k_x^-$ decreases this asymptotic value, thereby setting a new lower limit for the time scale of complete adaptation.

Thus, decoupling modes of feedback targeting an adaptor-proximal event propagates adaptation through an enzyme cascade only if the pathway also contains deactivators at each stage. However, the presence of deactivating enzymes alone does not produce adaptation under conditions of no feedback (even for high P_i^T:E_i^T). Therefore, in experimental studies of similar pathways, if overexpression of a deactivating enzyme such as a phosphatase shifts the corresponding kinase from a seemingly nonadaptive to adaptive signal, this shift is not attributable solely to phosphatase overexpression but also is suggestive of preexisting decoupling feedback mechanisms.

Upstream Effects: Comparison between Adaptor- versus Enzyme-Targeted Feedback. While the above results describing feedback targeting adaptor complex E_0* also apply to the case of enzyme-targeted feedback regulation, these two modes of feedback have differential effects on components *upstream* of the target. Under no-feedback conditions, the enzyme E_2 has transitory interaction with its upstream activator E_1*, which is released once the transition complex (E_1*E_2) dissociates. Thus, as a catalyst E_1* is both a reagent and product, resulting in no net consumption through interaction with its substrate E_2. Therefore, when enzyme E_2 is converted into its nonfunctional state E_2^- in the presence of feedback targeting E_2*, it has little effect on the steady-state level of upstream components E_1 and E_1* (Figure 10).

However, the adaptor complex E_0* derives from more stable association between C*A_1 and the second adaptor protein A_2. When E_0*-targeted feedback begins to drive the second adaptor protein into its nonfunctional state A_2^-, it shifts local association reactions in favor of distributing more of the first adaptor protein A_1 into the C*A_1 state. Thus, adaptor complex-targeted feedback propagates significant perturbations to upstream components, specifically resulting in higher steady-state levels (~20% greater) of complex-associated, first adaptor (C*A_1) than in the absence of feedback (Figure 10). This effect upstream of adaptor-targeted feedback has at least two important implications. First, because the incorporation of feedback yields a higher steady-state level of complex-associated, first adaptor C*A_1 than in its absence, the actual affinity ascribed to the interaction between activated receptors and the first adaptor protein (C* ↔ A_1) will be overestimated in systems containing this mode of feedback. Second, if the complex C*A_1 served as a branch point into another signaling pathway, a feedback-mediated increase in C*A_1 levels would heighten information transfer through this secondary pathway. This suggests that negative feedback, even though operating in isolation within a single pathway, can foster cross-talk between pathways, provided feedback targets an adaptor, not an enzyme, near an upstream signaling branch point.

Comparison with Experimental System and Data. ***Correspondence between Model Scheme and Experimental System.*** Since our model scheme (Figure 3) was designed as an approximation of the MAPK pathway, it offers a rigorous means to examine whether the mechanisms incorporated in our model predict features of ERK signaling dynamics consistent with our previous experi-

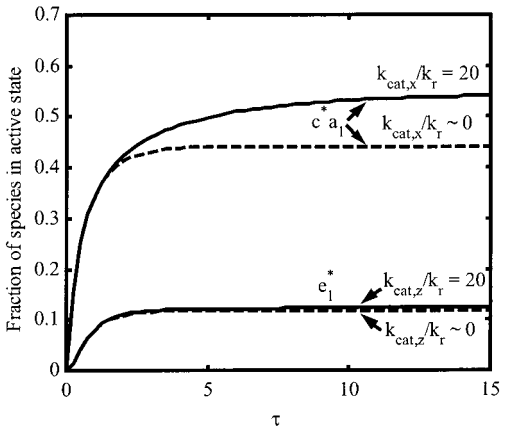

Figure 10. Comparison of effects upstream of adaptor- versus enzyme-targeted feedback. The components directly upstream of adaptor- and enzyme-targeted feedback are C^*A_1 and E_1^*, respectively. The fraction of adaptor A_1 associated with activated receptor−ligand complex (c^*a_1) is shown as a function of time in the top two curves under conditions where adaptor-targeted feedback is on ($k_{cat,x}/k_r = 20$) or off ($k_{cat,x}/k_r \approx 0$). Similarly, the time course of the fraction of first enzyme in its active state (e_1^*) is shown when enzyme-targeted feedback is on ($k_{cat,z}/k_r \approx 20$) or off ($k_{cat,z}/k_r \approx 0$). In contrast to enzyme-targeted feedback wherein there is no difference in the time course of signaling via the upstream component E_1^*, adaptor-targeted feedback propagates a significant effect upstream of feedback target. The steady-state level of signal c^*a_1 increases ~20% with the inclusion of adaptor-targeted feedback.

mental measurements. In addition to implementing activation and negative regulatory mechanisms known to exist in MAPK pathways, consideration of relevant experimental data justify approximations made in our model design (Asthagiri et al., 1999; Asthagiri et al., 2000).

While we incorporate deactivating enzymes such as phosphatases in our model, the total levels of these enzymes remain fixed and are not dynamically regulated through feedback mechanisms. However, transcriptional upregulation of phosphatases in response to ERK activation has been reported in some cell types (Brondello et al., 1997; Grumont et al., 1996). Importantly, this form of feedback operates over longer time scales. In our experimental Chinese hamster ovary (CHO) cell system, stimulation by either adhesion to fibronectin (Fn)-coated surfaces or binding of soluble mitogen insulin rapidly initiates an ERK2 signal, whose consequent deactivation begins within 10 min of stimulation and is complete by 20 min (Figure 11). Given this short duration of ERK2 activity, we have purposefully excluded delayed feedback mechanisms, while implementing feedback events that occur over time scales of relevance to the observed signal decay in our system.

It also should be noted that changing the mode of stimulation (Fn versus insulin) has no effect on the quantitative features of ERK2 signal decay (Figure 11). In both cases, signal decay is achieved within 20 min and is independent of signal intensity, demonstrating that the negative feedback mechanism(s) diminishing the signal is a property of the ERK2 pathway itself and not particular to the stimulus. Consistent with this observation, we have chosen an enzyme late in the cascade (E_4^*) as our feedback initiator and either the adaptor A_2 (in the complex E_0^*) or enzyme E_2^* as our feedback target, thereby self-containing the feedback loop within the MAPK pathway. Given these multiple points of correspondence between our model scheme and putative activation and feedback mechanisms governing ERK2 activity, this model was used to analyze further some crucial features of our experimental data.

Model Analysis of Experimental Findings. Three attributes of ERK2 signaling dynamics were observed in our experimental system (Asthagiri et al., 1999; Asthagiri et al., 2000). First, ERK2 activity always decays back to its basal level even though stimulus recognition (i.e., receptor−ligand binding) has reached a supra-basal steady-state level (Figure 11A). Thus, the ERK2 signal becomes desensitized to the continued presence of stimulus. Moreover, a second feature is that in some cases such as stimulation by adhesion to Fn, ERK2 signal not only decays in the presence of stimulus but also decays while stimulus recognition continues to increase (Figure 11B) in a form of desensitization that we have termed "ultra-desensitization". Finally, regardless of its relation to the kinetics of stimulus recognition, complete signal decay is typically achieved in 15−20 min. As demonstrated in a previous study, the rate of decay is independent of stimulus amount and is strictly proportional to the intensity of the ERK2 signal, demonstrating that this signal decay obeys first-order kinetics with respect to signal intensity. Here, we tested whether our model would predict signaling dynamics with features comparable to that observed in our experimental system.

First, we have already shown that implementing feedback targeting an adaptor complex E_0^* or an upstream enzyme E_2^* is sufficient to induce desensitization of signals downstream of the target, provided constitutive levels of deactivators (e.g., phosphatases) are present (Figure 7). In experiment, this decay occurred within ~20 min, corresponding to dimensionless time $\tau = 6$. As discussed above, equivalently rapid decay can be achieved in our model simulations, depending on values of critical dimensionless parameters such as the deactivator-to-activator ratio and feedback strength (Figure 9).

To investigate the relation between signal desensitization and stimulus recognition, we define a quantitative measure of desensitization (δ) as the ratio of time required for stimulus recognition or receptor−ligand binding to reach near (~98%) steady-state level to the time required for signal to attain its peak intensity. Values of δ greater than 1 (ultra-desensitization) reflect that the signal reaches its peak and begins to subside, even while stimulus recognition continues to occur. Under certain conditions, ultra-desensitization of a late signal in the cascade E_5^* is driven by adaptor-targeted feedback in our model (Figure 13). The signal's peak occurs when deactivation rate first begins to outweigh that of activation. At high $P_5^T:E_5^T$ ratio relatively greater deactivators than activators are present, so that signal deactivation occurs more rapidly, provided sufficient feedback is driving the decay process (high $k_x^+ E_4^T/k_x^-$). In this regime, deactivation rate outweighs activation rate earlier during signal propagation, thereby producing a signaling peak that precedes stimulus recognition ($\delta > 1$). Importantly, the strength with which feedback is driven ($k_x^+E_4^T/k_x^-$) determines if there exists any range of $P_5^T:E_5^T$ ratio yielding ultra-desensitization. At low $k_x^+E_4^T/k_x^-$ values, the rate at which feedback is initiated becomes limiting and even high levels of $P_5^T:E_5^T$ do not produce ultra-desensitization.

Finally, in addition to achieving complete signal adaptation, experimental observations showed that ERK2 signal decay obeys first-order kinetics with respect to signal intensity. To determine whether our model predicts similar kinetics, simulations were performed over a range of ligand amounts to assess the relationship

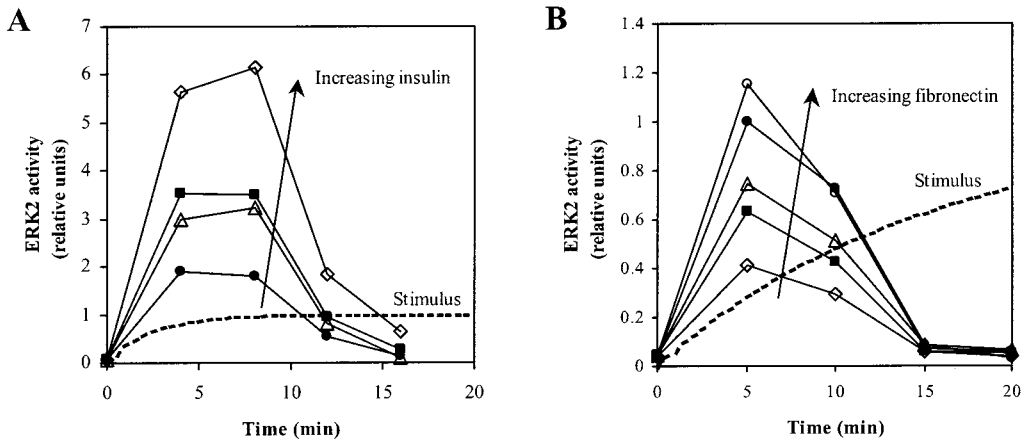

Figure 11. Features of ERK2 signal adaptation in an experimental CHO cell system. CHO cell stimulation by either (A) recognition of soluble factor insulin [1 (●), 10 (△, 100 (■), 1000 (◊) nM] or (B) adhesion to fibronectin-coated surfaces [5.3 (◊), 10 (■), 25 (△), 50 (○), 310 (●) × 10^7/mm^2; corresponding coating concentrations: 0.1, 0.25, 0.5, 1, 10 μg/mL] induces a transient ERK2 signal (Asthagiri et al., 1999; Asthagiri et al., 2000). While stimulation by insulin imparts stronger ERK2 activation, both ligands elicit an ERK2 signal that reaches its peak at ca. 5−10 min and subsides back to a basal level within 15−20 min. A comparison of the signaling time course and the kinetics of stimulus recognition (i.e., receptor−ligand binding) is offered by the visual observation that receptor-mediated recognition of fibronectin (as approximated by cell spreading on the substratum) is a gradual process that reaches steady state at ~60 min after initial exposure. Utilizing a characteristic time constant from this qualitative observation, a stimulus recognition curve (as a fraction of steady-state recognition level) is derived for the fibronectin case (dotted line, B). Similarly, for the case of insulin, using literature-reported values $k_f = 10^7$ M^{-1} min^{-1} and $k_r = 0.2$ min^{-1} (Lipkin et al., 1986) and setting $L_0 = K_d$ ($K_d = k_r/k_f$), the time course of insulin detection is plotted as the stimulus curve in panel A, assuming simple second-order association and first-order dissociation kinetics. It is evident that in the case of fibronectin stimulation, signal decay occurs not only in the presence of stimulus (as is the case with insulin), but also while stimulus recognition continues to *increase*.

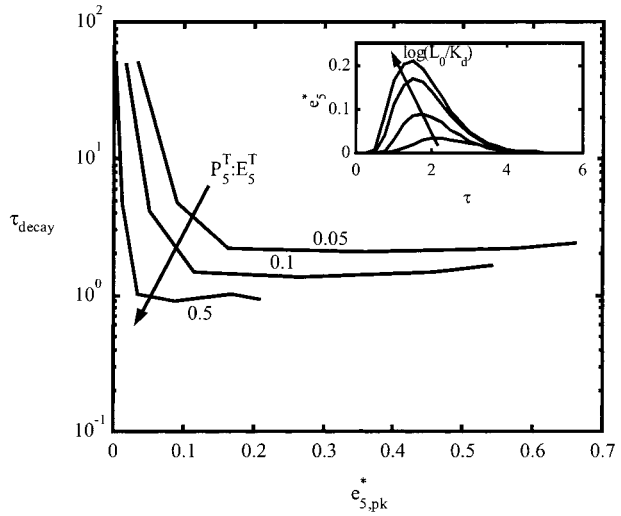

Figure 12. Relation between kinetics of signal decay and signal intensity. For a given dose of ligand, the signal intensity of the final enzyme in the cascade was quantified as the maximum fraction to which it is activated before its complete adaptation. As ligand concentration is increased over a range of log(L_0/K_d) = −3 to 1, signal intensity $e^*_{5,pk}$ increases. Concurrent with this increase, the time required for signal adaptation τ_{decay} decreases until reaching a lower asymptotic limit, at which point τ_{decay} remains constant despite increasing signal intensity. As shown in the inset, the time course of signal e_5* reveals that signal decays to a basal level within the same amount of time regardless of stimulus amount or signal intensity in this asymptotic limit. Thus, the rate of signal decay obeys lumped, first-order kinetics with respect to signal intensity in this regime. The asymptotic limit for the time scale of decay is reduced by increasing the deactivator:activator ratio at the fifth stage of the cascade.

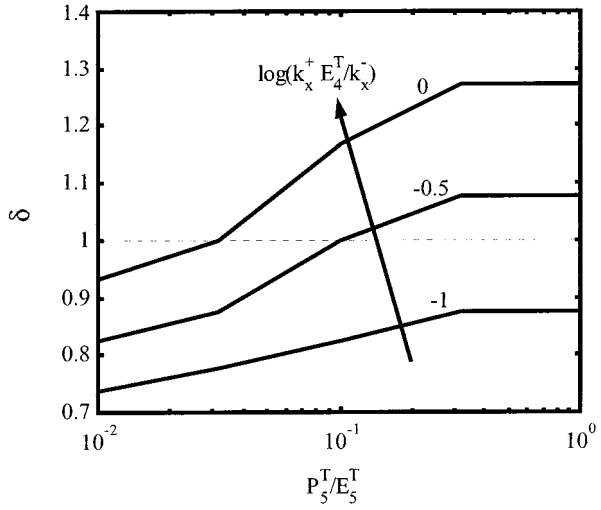

Figure 13. Decoupling feedback induces ultra-desensitization. The desensitization factor (δ) for a signal late in the enzyme cascade is shown as a function of deactivator:activator ratio at that stage (P_5^T:E_5^T) for different levels of feedback strength ($k_x^+ E_4^T/k_x^-$). Ultra-desensitization corresponds to values of δ greater than 1. While higher deactivator:activator ratios increases the desensitization factor, its value rises above 1 only under sufficiently high feedback strength.

between intensity of signaling via activation of enzyme E_5*, which is situated late in the cascade in a manner analogous to ERK2, and the time required for feedback-mediated decay of this signal. If adaptation followed "lumped", first-order kinetics with respect to signal intensity, the time scale of adaptation τ_{decay} would be insensitive to changes in signal intensity as quantified by the maximum level ($e_{5,pk}$*) to which enzyme E_5 is activated in response to ligand stimulation. As shown in Figure 12, for a given level of deactivator:activator ratio at the fifth stage, the time scale of decay decreases monotonically with increasing signal intensity until reaching a lower asymptotic value, at which point τ_{decay} becomes independent of signal intensity. At this asymptotic limit, signal decay is achieved in the same amount of time despite elevations in signal intensity caused by higher ligand doses (inset of Figure 12), exactly as observed in our experimental system (Figure 11). In this regime, signal decay behaves with lumped, first-order dependence on signal intensity. Moreover, the asymptotic

value of τ_{decay} is prescribed partly by the ratio of deactivator to activator enzymes at that stage of the cascade. As this ratio is increased, a higher relative amount of deactivator is present to deactivate the signal at a faster rate, thereby reducing the lower limit for adaptation time.

Conclusions

Overall, we believe that our computational study of feedback in a model MAPK pathway will help increase understanding of the diverse dynamic behavior that this important signaling cascade can exhibit. Our model delineates the role of regulatory elements in producing rapid adaptation not only of species directly targeted by feedback but also of signals further downstream. Moreover, it elucidates the novel concept that negative feedback can enhance an upstream signal, thereby potentially fostering cross-talk into alternative pathways interconnected at such an enhanced upstream component. This modeling approach provides further support for viewing signaling networks in terms of system dynamics and control theoretical frameworks (Asthagiri and Lauffenburger, 2000; Lauffenburger, 2000; Yi et al., 2000).

Acknowledgment

The authors gratefully acknowledge support from an Anna Fuller Fellowship in Molecular Oncology from the MIT Cancer Research Center (A.R.A.) and NIH grant GM-53905 (D.A.L.).

Appendix: Model Equations

The early steps in signal processing involving the recognition of ligand L and eventual formation of a signaling-competent, receptor−ligand complex (C*) are described by the following rate expressions:

$$\frac{dc}{d\tau} = \left(\frac{L_0}{k_r/k_f}\right) rl - c - 2\left(\frac{R_0}{k_r/k_c}\right) c^2 + 2\left(\frac{k_u}{k_r}\right) c_2 \quad \text{(A1)}$$

$$\frac{dc_2}{d\tau} = \left(\frac{R_0}{k_r/k_c}\right) c^2 - \left(\frac{k_u}{k_r}\right) c - \left(\frac{k_c^+}{k_r}\right) c_2 + \left(\frac{k_c^-}{k_r}\right) c^* \quad \text{(A2)}$$

The rate expression for species C* also includes terms describing its interaction with adaptors A_1 and A_2 to form complexes C^*A_1 or E_0^*:

$$\frac{dc^*}{d\tau} = \left(\frac{k_c^+}{k_r}\right) c_2 - \left(\frac{k_c^-}{k_r}\right) c^* - \left(\frac{k_f^{\,1} A_1^T}{k_r}\right) (c^*)(a_1) + \left(\frac{k_r^{\,1}}{k_r}\right)\left(\frac{A_1^T}{R_0}\right)(c^* a_1) - \left(\frac{k_f^{\,12} A_1^T}{k_r}\right)(c^*)(a_1 a_2) + \left(\frac{k_r^{\,12}}{k_r}\right)\left(\frac{A_2^T}{R_0}\right) e_0^* \quad \text{(A3)}$$

Rate expressions for adaptor−receptor complexes such as C^*A_1 and E_0^* also include effects from adaptor-targeted feedback catalyzed by active enzyme E_4^*:

$$\frac{d(c^* a_1)}{d\tau} = \left(\frac{k_f^{\,1} R_0}{k_r}\right)(c^*)(a_1) - \left(\frac{k_r^{\,1}}{k_r}\right)(c^* a_1) - \left(\frac{k_f^{\,2} A_2^T}{k_r}\right)(c^* a_1)(a_2) + \left(\frac{k_r^{\,2}}{k_r}\right)\left(\frac{A_2^T}{A_1^T}\right) e_0^* + \left(\frac{k_{cat,x}}{k_r}\right)\left(\frac{E_4^T}{A_1^T}\right)(e_0^* e_4^*) \quad \text{(A4)}$$

$$\frac{de_0^*}{d\tau} = \left(\frac{k_f^{\,2} A_1^T}{k_r}\right)(c^* a_1)(a_2) - \left(\frac{k_r^{\,2}}{k_r}\right) e_0^* + \left(\frac{k_f^{\,12} A_1^T}{k_r}\right)(c^*)(a_1 a_2) - \left(\frac{k_r^{\,12}}{k_r}\right) e_0^* - \left(\frac{k_1^+ E_1^T}{k_r}\right)(e_0^*)(e_1) + \left(\frac{k_1^- + k_{cat,1}}{k_r}\right)\left(\frac{E_1^T}{A_2^T}\right)(e_1 e_0^*) - \left(\frac{k_x^+ E_4^T}{k_r}\right)(e_0^*)(e_4^*) + \left(\frac{k_x^-}{k_r}\right)\left(\frac{E_4^T}{A_2^T}\right)(e_0^* e_4^*) \quad \text{(A5)}$$

Completing equations involving adaptors A_1 and A_2, we include rate expressions that accommodate interactions between free adaptors to form the heteroadaptor complex A_1A_2 and the feedback-mediated production of a signaling-defective adaptor species A_2^- incapable of engaging the first adaptor A_1:

$$\frac{d(a_1 a_2)}{d\tau} = -\left(\frac{k_f^{\,12} R_0}{k_r}\right)(c^*)(a_1 a_2) + \left(\frac{k_r^{\,12}}{k_r}\right)\left(\frac{A_2^T}{A_1^T}\right) e_0^* + \left(\frac{k_c^{\,12} A_2^T}{k_r}\right)(a_1)(a_2) - \left(\frac{k_d^{\,12}}{k_r}\right)(a_1 a_2) \quad \text{(A6)}$$

$$\frac{da_2^-}{d\tau} = \left(\frac{k_{cat,x}}{k_r}\right)\left(\frac{E_4^T}{A_2^T}\right)(e_0^*\, e_4^*) \quad \text{(A7)}$$

These species also perform under mass-balance constraints. For those components involved in ligand recognition and receptor−adaptor interactions, these balances are given by

$$1 = r + c + 2\left(c_2 + c^* + \left(\frac{A_1^T}{R_0}\right)(c^* a_1) + \left(\frac{A_2^T}{R_0}\right) e_0^* + \left(\frac{E_4^T}{R_0}\right)(e_0^* e_4^*) + \left(\frac{E_1^T}{R_0}\right)(e_1 e_0^*)\right) \quad \text{(A8)}$$

$$(1 - l)\left(\frac{N_A L_0}{n R_0}\right) = c + 2\left(c_2 + c^* + \left(\frac{A_1^T}{R_0}\right)(c^* a_1) + \left(\frac{A_2^T}{R_0}\right) e_0^* + \left(\frac{E_4^T}{R_0}\right)(e_0^* e_4^*) + \left(\frac{E_1^T}{R_0}\right)(e_1 e_0^*)\right) \quad \text{(A9)}$$

$$1 = a_1 + (c^* a_1) + (a_1 a_2) + \left(\frac{A_2^T}{A_1^T}\right) e_0^* + \left(\frac{E_4^T}{A_1^T}\right)(e_0^*\, e_4^*) + \left(\frac{E_1^T}{A_1^T}\right)(e_1 e_0^*) \quad \text{(A10)}$$

$$1 = a_2 + \left(\frac{A_1^T}{A_2^T}\right)(a_1 a_2) + e_0^* + \left(\frac{E_4^T}{A_2^T}\right)(e_0^*\, e_4^*) + \left(\frac{E_1^T}{A_2^T}\right)(e_1 e_0^*) + a_2^- \quad \text{(A11)}$$

Within the enzyme cascade, most equations are similar for each stage, except in cases of stages $i = 2$ and 4, since these stages are subject to or are engaged in feedback pathways. First, we write the mass balance constraints on signaling enzymes E_i and their respective deactivators P_i:

$$1 = e_i + (e_i e_{i-1}^*) + e_i^* + \left(\frac{E_{i+1}^T}{E_i^T}\right)(e_{i+1} e_i^*) + \left(\frac{P_i^T}{E_i^T}\right)(e_i p_i) \quad \text{for } i = 1, 3, \text{ and } 5 \quad \text{(A12)}$$

$$1 = p_i + (e_i^* p_i) \text{ for all } i \quad \text{(A13)}$$

For the 2nd and 4th stages, the mass balance on signaling enzymes E_2 and E_4 are

$$1 = e_2 + e_2^* + e_2^- + (e_2 e_1^*) + \left(\frac{E_3^T}{E_2^T}\right)(e_3 e_2^*) + \left(\frac{P_2^T}{E_2^T}\right)(e_2^* p_2) + \left(\frac{E_4^T}{E_2^T}\right)(e_2^* e_4^*), \text{ and} \quad \text{(A14)}$$

$$1 = e_4 + e_4^* + (e_4 e_3^*) + \left(\frac{E_5^T}{E_4^T}\right)(e_5 e_4^*) + \left(\frac{P_4^T}{E_4^T}\right)(e_4^* p_4) + (e_0^* e_4^*) + (e_2^* e_4^*) \quad \text{(A15)}$$

In order for each activate enzyme E_i^* to be converted back to its inactive state E_i, it forms a transition complex with its corresponding deactivator P_i as described by the following:

$$\frac{d(e_i^* p_i)}{d\tau} = \left(\frac{k_{P_i}^+ E_i^T}{k_r}\right)(e_i^*)(p_i) - \left(\frac{k_{P_i}^-}{k_r} + \frac{k_{\text{cat},P_i}}{k_r}\right)(e_i^* p_i) \quad \text{for all } i \quad \text{(A16)}$$

A similar equation can be written for the enzyme−substrate transition complex formed when each enzyme E_i is activated by the previous enzyme in the cascade E_{i-1}^*:

$$\frac{d(e_i e_{i-1}^*)}{d\tau} = \left(\frac{k_i^+ E_{i-1}^T}{k_r}\right)(e_i)(e_{i-1}^*) - \left(\frac{k_i^-}{k_r} + \frac{k_{\text{cat},i}}{k_r}\right)(e_i e_{i-1}^*) \quad \text{for all } i \text{ and where } E_0^T \equiv A_2^T \quad \text{(A17)}$$

Two other enzyme−substrate transition complexes occur as a result of feedback regulation:

$$\frac{d(e_2^* e_4^*)}{d\tau} = \left(\frac{k_z^+ E_2^T}{k_r}\right)(e_4^*)(e_2^*) - \left(\frac{k_z^-}{k_r} + \frac{k_{\text{cat},z}}{k_r}\right)(e_2^* e_4^*) \text{ and} \quad \text{(A18)}$$

$$\frac{d(e_0^* e_4^*)}{d\tau} = \left(\frac{k_x^+ A_2^T}{k_r}\right)(e_4^*)(e_0^*) - \left(\frac{k_x^-}{k_r} + \frac{k_{\text{cat},x}}{k_r}\right)(e_0^* e_4^*) \quad \text{(A19)}$$

As adaptor-targeted feedback produces species A_2^-, enzyme-targeted feedback converts E_2^* into a "signaling-dead" form E_2^-:

$$\frac{de_2^-}{d\tau} = \left(\frac{k_{\text{cat},z}}{k_r}\right)\left(\frac{E_4^T}{E_2^T}\right)(e_2^* e_4^*) \quad \text{(A20)}$$

Finally, these activation, deactivation, and feedback processes regulate the level of active enzyme E_i^*. Rates of change of these species for each stage is given by

$$\frac{de_i^*}{d\tau} = \left(\frac{k_{i,\text{cat}}}{k_r}\right)(e_i e_{i-1}^*) - \left(\frac{k_{i+1}^+ E_{i+1}^T}{k_r}\right)(e_i^*)(e_{i+1}) + \left(\frac{k_{i+1}^- + k_{\text{cat},i+1}}{k_r}\right)\left(\frac{E_{i+1}^T}{E_i^T}\right)(e_{i+1} e_i^*) - \left(\frac{k_{P_i}^+ P_i^T}{k_r}\right)(e_i^*)(p_i^*) + \left(\frac{k_{P_i}^-}{k_r}\right)\left(\frac{P_i^T}{E_i^T}\right)(e_i^* p_i) \text{ for } i = 1,3, \text{ and } 5 \quad \text{(A21)}$$

For the 2nd stage, the rate expression includes depletion of active enzyme E_2^* by enzyme-targeted feedback:

$$\frac{de_2^*}{d\tau} = \left(\frac{k_{2,cat}}{k_r}\right)(e_2 e_1^*) - \left(\frac{k_3^+ E_3^T}{k_r}\right)(e_2^*)(e_3) + \left(\frac{k_3^- + k_{\text{cat},3}}{k_r}\right)\left(\frac{E_3^T}{E_2^T}\right)(e_3 e_2^*) - \left(\frac{k_{P_2}^+ P_2^T}{k_r}\right)(e_2^*)(p_2^*) + \left(\frac{k_{P_2}^-}{k_r}\right)\left(\frac{P_2^T}{E_2^T}\right)(e_2^* p_2) - \left(\frac{k_z^+ E_4^T}{k_r}\right)(e_2^*)(e_4^*) + \left(\frac{k_z^-}{k_r}\right)\left(\frac{E_4^T}{E_2^T}\right)(e_2^* e_4^*) \quad \text{(A22)}$$

The 4th stage incorporates the involvement of the feedback initiator E_4^* in both feedback modes:

$$\frac{de_4^*}{d\tau} = \left(\frac{k_{\text{cat},4}}{k_r}\right)(e_4 e_3^*) - \left(\frac{k_5^+ E_5^T}{k_r}\right)(e_4^*)(e_5) + \left(\frac{k_5^- + k_{\text{cat},5}}{k_r}\right)\left(\frac{E_5^T}{E_4^T}\right)(e_5 e_4^*) - \left(\frac{k_{P_4}^+ P_4^T}{k_r}\right)(e_4^*)(p_4^*) + \left(\frac{k_{P_4}^-}{k_r}\right)\left(\frac{P_4^T}{E_4^T}\right)(e_4^* p_4) - \left(\frac{k_x^+ A_2^T}{k_r}\right)(e_0^*)(e_4^*) + \left(\frac{k_x^-}{k_r} + \frac{k_{\text{cat},x}}{k_r}\right)(e_0^* e_4^*) - \left(\frac{k_z^+ E_2^T}{k_r}\right)(e_2^*)(e_4^*) + \left(\frac{k_z^-}{k_r} + \frac{k_{\text{cat},z}}{k_r}\right)(e_2^* e_4^*) \quad \text{(A23)}$$

Estimations of Parameter Values. Typical values for parameters described in the model schematic and used in model equations are shown in Table 2, and references provided therein highlight the sources for these values. In this section, we provide only discussion of any calculations necessary to modify parameters for application in our model. Coupling and association steps between two species in the membrane (as in the case of dimerization) or between a membrane-associated and cytosolic species were assumed to be diffusion-limited (Haugh and Lauffenburger, 1997). Units for rate constants for intramembrane dimerization reaction were adjusted to incorporate three-dimensional units of volume by using the height of membrane space and the surface area of the cell (Lauffenburger and Linderman, 1993). Interactions among adaptors and the phosphorylated receptor−ligand complex are recognized as forming a cycle whose thermodynamic constraint reduces the degrees of freedom in defining these rate constants:

$$\left(\frac{k_r^1}{k_f^1}\right)\left(\frac{k_r^2}{k_f^2}\right)\left(\frac{k_f^{12}}{k_r^{12}}\right)\left(\frac{k_c^{12}}{k_d^{12}}\right) = 1 \qquad \text{(A24)}$$

References and Notes

Alon, U.; Surette, M. G.; Barkai, N.; Leibler, S. Robustness in bacterial chemotaxis. *Nature* **1999**, *397*, 168−171.

Anderson, N. G.; Li, P.; Marsden, L. A.; Williams, N. T.; Roberts, M.; Sturgill. T. W. Raf-1 is a potential substrate for mitogen-activated protein kinase in vivo. *Biochem. J.* **1991**, *277*, 573−576.

Aronheim, A., D.; Engelber, N.; Li, N.; Al-Alawi, J.; Schlessinger; Karin, M. Membrane targeting of the nucleotide exchange factor Sos is sufficient for activating the Ras signaling pathway. *Cell* **1994**, *78*, 949−961.

Asthagiri, A. R.; Nelson, C. M.; Horwitz, A. F.; Lauffenburger, D. A. Quantitative relationship among integrin-ligand binding, adhesion, and signaling via focal adhesion kinase and extracellular signal-regulated kinase 2. *J. Biol. Chem*. **1999**, *274*, 27119−27127.

Asthagiri, A. R.; Lauffenburger, D. A. Bioengineering models of cell signaling. *Annu. Rev. Biomed. Eng.* **2000**, *2*, 31−53.

Asthagiri, A. R.; Reinhart, C. A.; Horwitz, A. F.; Lauffenburger, D. A. The role of transient ERK2 signals in fibronectin- and insulin-mediated DNA synthesis. *J. Cell Sci.* **2000**, *113*, 4499−4510.

Barkai, N.; Leibler, S. Robustness in simple biochemical networks. *Nature* **1997**, *387*, 913−7.

Brondello, J. M.; Brunet, A.; Pouyssegur, J.; McKenzie. F. R. The dual specificity mitogen-activated protein kinase phosphatase-1 and -2 are induced by the p42/p44MAPK cascade. *J. Biol. Chem*. **1997**, *272*, 1368−1376.

Brunet, A.; Pages, G.; Poussegur, J. Growth factor-stimulated MAP kinase induces rapid retrophosphorylation and inhibition of MAP kianse kinase (MEK1). *FEBS Lett.* **1994**, *346*, 299−303.

Buday, L.; Warne, P. H.; Downward, J. Downregulation of the Ras activation pathway by MAP kinase phosphorylation of Sos. *Oncogene* **1995**, *11*, 1327−1331.

Chen, D.; Waters, S. B.; Holt, K. H.; Pessin, J. E. Sos phosphorylation and disassociation of the Grb2-Sos complex by the ERK and JNK signaling pathways. *J. Biol. Chem*. **1996**, *271*, 6328−6332.

Corbalan-Garcia, S.; Yang, S.-S.; Degenhardt, K. R.; Bar-Sagi, D. Identification of the mitogen-activated protein kinase phosphorylation sites on human Sos1 that regulate interaction with Grb2. *Mol. Cell. Biol.* **1996**, *16*, 5674−5682.

Davis, R. J. The mitogen-activated protein kinase signal transduction pathway. *J. Biol. Chem*. **1993**, *268*, 14553−14556.

DeGregori, J.; Kowalik, T.; Nevins, J. R. Cellular targets for activation by the E2F1 transcription factor include DNA synthesis- and G1/S-regulatory genes. *Mol. Cell Biol.* **1995**, *15*, 4215−4224.

Douville, E.; Downward, J. EGF induced Sos phosphorylation in PC12 cells involves p90 Rsk-2. *Oncogene* **1997**, *15*, 373−383.

Ferrell, J. E., Jr. Tripping the switch fantastic: how a protein kinase cascade can convert graded inputs into switch-like outputs. *TIBS* **1996**, *21*, 460−466.

Girard, F.; Strausfeld, U.; Fernandez, A.; Lamb, N. J. C. Cyclin A is required for the onset of DNA replication in mammalian fibroblasts. *Cell* **1991**, *67*, 1169−1179.

Grumont, R. J.; Rasko, J. E.; Strasser, A.; Gerondakis, S. Activation of the mitogen-activate protein kinase pathway induces transcription of the PAC-1 phosphatase gene. *Mol. Cell. Biol.* **1996**, *16*, 2913−2921.

Hanks, S. K.; Polte, T. R. Signaling through focal adhesion kinase. *Bioessays* **1997**, *19*, 137−145.

Haugh, J. M.; Lauffenburger, D. A. Physical modulation of intracellular signaling processes by locational regulation. *Biophys. J.* **1997**, *72*, 2014−2031.

Huang, C.-Y. F.; Ferrell, J. E., Jr. Ultrasensitivity in the mitogen-activated protein kinase cascade. *Proc. Natl. Acad. Sci. U.S.A.* **1996**, *93*, 10078−10083.

Joneson, T.; Bar-Sagi, D. Ras effectors and their role in mitogenesis and oncogenesis. *J. Mol. Med.* **1997**, *75*, 587−593.

Kao, C. M. Functional genomic technologies: creating new paradigms for fundamental and applied biology. *Biotechnol. Prog.* **1999**, *15*, 304−311.

Keyse, S. M. Protein phosphatases and the regulation of mitogen-activated protein kinase signaling. *Curr. Op. Cell. Biol.* **2000**, *12*, 186−192.

Kholodenko, B. N.; Demin, O. V.; Moehren, G.; Hoek, J. B. Quantification of short OLINIT-term signaling by the epidermal growth factor receptor. *J. Biol. Chem*. **1999**, *274*, 30169−30181.

Koshland, D. E., Jr.; Goldbeter, A.; Stock, J. B. Amplification and adaptation in regulatory and sensory systems. *Science* **1982**, *217*, 220−225.

Langlois, W. J.; Sasaoka, T.; Saltiel, A. R.; Olefsky, J. M. Negative feedback regulation and desensitization of insulin- and epidermal growth factor-stimulated p21ras activation. *J. Biol. Chem*. **1995**, *270*, 25320−25323.

Lauffenburger, D. A.; Linderman, J. J. *Receptors: Models for Binding, Trafficking, and Signaling.* Oxford University Press: New York, 1993.

Lauffenburger, D. A. Cell signaling pathways as control modules: complexity for simplicity? *Proc. Natl. Acad. Sci. U.S.A.* **2000**, *97*, 5031−5033.

Leevers, S. J.; Paterson, H. F.; Marshall, C. J. Requirement for Ras in Raf activation is overcome by targeting Raf to the plasma membrane. *Nature* **1994**, *369*, 411−414.

Levchenko, A.; Bruck, J.; Sternber, P. W. Scaffold proteins may biphasically affect the levels of mitogen-activated protein kinase signaling and reduce its threshold properties. *Proc. Natl. Acad. Sci. U.S.A.* **2000**, *97*, 5818−5823.

Levitzki, A. Targeting signal transduction for disease therapy. *Curr. Op. Cell. Biol.* **1996**, *8*, 239−244.

Lewis, T. S.; Shapiro, P. S.; Ahn, N. G. Signal transduction through MAP kinase cascades. *Adv. Cancer Res.* **1998**, *74*, 49−139.

Lipkin, E. W.; Teller, D. C.; de Haen, C. Kinetics of insulin binding to rat white fat cells at 15 C. *J. Biol. Chem*. **1986**, *261*, 1702−1711.

Maemura, M.; Iino, Y.; Koibuchi, Y.; Yokoe, T.; Morishita, Y. Mitogen-activated protein kinase cascade in breast cancer. *Oncology* **1999**, *57*, 37−44.

Marshall, C. J. Specificity of receptor tyrsosine kinase signaling: transient versus sustained extracellular signal-regulated kinase activation. *Cell* **1995**, *80*, 179−185.

Mineo, C.; Anderson, R. G. W.; White, M. A. Physical association with Ras enhances activation of membrane-bound Raf (Raf-CAAX). *J. Bio. Chem*. **1997**, *272*, 10345−10348.

Roovers, K.; Davey, G.; Zhu, X.; Bottazzi, M. E.; Assoian, R. K. $\alpha 5\beta 1$ integrin controls cyclin D1 expression by sustaining mitogen-activated protein kinase activity in growth factor-treated cells. *Mol. Biol. Cell* **1999**, *10*, 3197−3204.

Roovers, K.; Assoian, R. K. Integrating the MAP kinase signal into the G1 phase cell cycle machinery. *Bioessays* **2000**, *22*, 818−826.

Rozakis-Adcock, M.; Fernley, R.; Wade, J.; Pawson, T.; Bowtell, D. The SH2 and SH3 domains of mammalian Grb2 couple the EGF receptor to the Ras activator mSos1. *Nature* **1993**, *363*, 83−85.

Schulze, A.; Zerfass-Thome, K.; Berges, J.; Middendorp, S.; Jansen-Durr, P.; Henglein, B. Anchorage-dependent transcription of the cyclin A gene. *Mol. Cell. Biol.* **1996**, *16*, 4632−4638.

Stokoe, D.; Macdonald, S. G.; Cadwallader, K.; Symons, M.; Hancock, J. F. Activation of Raf as a result of recruitment to the plasma membrane. *Science* **1994**, *264*, 1463−1467.

Tombes, R. M.; Auer, K. L.; Mikkelsen, R.; Valerie, K.; Wymann, M. P.; Marshall, C. J.; McMahon, M.; Dent, P. The mitogen-activated protein (MAP) kinase cascade can either stimulate or inhibit DNA synthesis in primary cultures of rat hepatocytes depending upon whether its activation is acute/phasic or chronic. *Biochem. J.* **1998**, *330*, 1451−1460.

van der Geer, P.; Hunter, T. Receptor protein-tyrosine kinases and their signal transduction pathways. *Annu. Rev. Cell Biol.* **1994**, *10*, 251−337.

Wartmann, M.; Hofer, P.; Turowski, P.; Saltiel, A. R.; Hynes, N. E. Negative modulation of membrane localization of the Raf-1 protein kinase by hyperphosphorylation. *J. Biol. Chem.* **1997**, *272*, 3915−3923.

Yi, T.-M.; Huang, Y.; Simon, M. I.; Doyle, J. Robust perfect adaptation in bacterial chemotaxis through integral feedback control. *Proc. Natl. Acad. Sci. U.S.A.* **2000**, *97*, 4649−4653.

Accepted for publication January 16, 2001.

BP010009K